Desalination and Water Treatment
www.deswater.com
doi: 10.1080/19443994.2013.821037

52 (2014) 6430–6439
October

Taylor & Francis
Taylor & Francis Group

Enhancing adsorption of Pb (II) and Cu (II) ions onto chitosan using tri-sodium citrate and epichlorohydrin as cross-linkers

Yanfang Sun, Yun Liu*, Yun Yang, Jianjun Li

Department of Chemistry, School of Science, Xi'an Jiaotong University, Xi'an 710049, China
Tel. +86 29 82655169; email: liuyun66@xjtu.edu.cn

Received 26 March 2013; Accepted 13 June 2013

ABSTRACT

In this study, tri-sodium citrate (CA), a chelating agent of low-cost and non-toxicity, was used together with epichlorohydrin (ECH) to cross-link chitosan (CTS) for enhancing the adsorption of Pb (II) and Cu (II) ions onto CTS. The chemical structure changes of the cross-linked CTS and metal ions-loaded absorbent were confirmed by thermogravimetric analysis, FTIR spectroscopy and X-ray diffraction. The effects of these factors, such as pH, temperature, contact time, and initial concentration of metal ions on the adsorption of Pb (II) and Cu (II) ions onto CTS–CA–ECH beads were investigated. The adsorption kinetics was evaluated utilizing pseudo-first-order and pseudo-second-order (PSO) models, the results indicated that the adsorption process fit well with the PSO kinetic model. Meanwhile, adsorption equilibrium isotherms were examined by Langmuir and Freundlich models, the results showed that the experimental data agreed well with Langmuir models and the maximum adsorption capacities were 121.95 and 151.52 $mg\,g^{-1}$ for Pb (II) and Cu (II) ions, respectively. Furthermore, desorption and regeneration tests indicated that ethylenediamine tetra-acetic acid could effectively regenerate the metal ions loaded CTS–CA–ECH beads, suggesting that the currently prepared adsorbent possessed an excellent reusability for the adsorption of Pb (II) and Cu (II) ions.

Keywords: Chitosan; Tri-sodium citrate; Chelating; Adsorption; Reuse

1. Introduction

In recent years, much attention has been focused on the contamination of aquatic media by heavy metals, because heavy metals are highly toxic even at low concentrations and can accumulate in living organisms, causing various disorders and diseases [1]. Several methods have been attempted to remove heavy metals from waste water such as chemical precipitation, filtration, membrane separation, electrochemical treatment, ion exchange, and adsorption [2–4]. Among these methods, adsorption is the most effective, especially when the heavy metal ions are present at low concentration in the wastewater. Although activated carbon is one of the most widely used adsorbent [5], because of its cost, more and more studies are concentrated on low-priced adsorbent from natural resources [2].

In particular, chitosan (CTS) is well established as an excellent natural adsorbent because its amino and hydroxyl groups may serve as coordination sites to form complexes with various heavy metal ions [6].

*Corresponding author.

Besides, CTS has many other useful features, for instance, abundance, nontoxicity, hydrophilicity, biocompatibility, etc. [1,7,8]. However, the application of CTS is largely limited due to its poor mechanical strength and chemical stability. To improve the performance of CTS, further chemical modification, such as cross-linking, grafting, and so on, is necessary. The cross-linking procedures are usually performed by the reaction of CTS with different cross-linker such as glutaraldehyde (GLA), ethylene glycol diglycidyl ether (EGDE), epichlorohydrin (ECH), and tripolyphosphate (TPP) [7–10].

ECH is a widely used cross-linking agent [7,11,12], it can form covalent bonds with nucleophilic groups such as hydroxyl groups and amino groups in polymers due to its reactive epoxide ring and chlorine atom.

TPP is a phosphorus-containing multivalent ionic cross-linker used to modify CTS into an excellent adsorbent of heavy metal ions in the previous reports [7,13]. However, it was found that phosphate discharged or escaped into water could cause secondary water contamination problems, such as excessively nourishing, algae blooming [14], oxygen deficiency, etc. developing harmful effects on aquatic organisms. Thus, cross-linking agents with less toxic characteristics are preferred nowadays. Tri-sodium citrate (CA), a chelating agent with three carboxylic anions, is extremely expected as a substitute for TPP in cross-linking CTS due to its nontoxicity, low-cost, and biodegradability.

In the current strategy, we attempted to modify CTS using trisodium citrate and ECH by ionic and covalent cross-linking for improving the adsorption ability of CTS toward Pb (II) and Cu (II) ions from aqueous solution. In addition, the chemical structure changes of the cross-linked CTS and metal ions-loaded absorbent were confirmed by thermogravimetric analysis (TGA), FTIR spectroscopy, and X-ray diffraction (XRD), and the adsorption kinetics and adsorption equilibrium isotherms were thoroughly investigated. Desorption and regeneration of the modified CTS were also examined.

2. Experimental

2.1. Materials

CTS with 40–100 mesh, 90–95% degree of deacetylation was purchased from Shanghai Sangon Biological Engineering & Technology. All other chemicals (lead nitrate, copper nitrate, trisodium citrate, and ECH) were of analytical grade. All aqueous solutions used in the following experiments were prepared using deionized water.

2.2. Measurements

TGA was conducted on NETZSCH TG-209C with heating rate of 20 °C min^{-1} and temperature range of 25–800 °C in the nitrogen flow. Spectroscopic analysis was carried out on a Nicolet Avatar 330 FTIR with KBr in the range of 4,000–500 cm^{-1}. XRD analysis was obtained by RIGAKU D/MAX-2400 with scanning scope of 2–50 °C and scanning speed of 2 °C min^{-1}. The concentrations of Pb (II) and Cu (II) ions were determined by flame atomic adsorption spectroscopy (FAAS) using an AA6000 spectrometer.

2.3. Cross-linking of CTS

Chitosan–citrate (CTS–CA) beads were prepared referenced to the previous literatures [13,15,16]. Briefly, 2.0 g of CTS powder was dissolved in 100 mL of 2% (v/v) acetic acid solution, and the solution was left for 24 h at room temperature to ensure there was no bubble in it. Then the viscous CTS solution was dropped using a syringe into a gently shaken trisodium citrate solution 10% (w/v), whose pH was adjusted to 6.0 to obtain gelled CTS–CA beads via forming ionic bonds, then the newly formed CTS–CA beads were kept in citrate solution at 4 °C for 1 h to increase their strength. Subsequently, the CTS–CA beads were collected by filtering the solution and washed extensively with distilled water to remove any sodium citrate residue. Afterward, the wet CTS–CA beads were added into 100 mL of 0.1 mol L^{-1} ECH solution, and the mixture was stirred at room temperature for 24 h at pH 6.0 [5]. The resultant beads (designated as CTS–CA–ECH) were filtered and washed several times with distilled water to remove any unreacted ECH, and then dried at 60 °C for 24 h. The CTS–CA–ECH beads were ground and sieved to a constant particle size (<200 μm) before use. Fig. 1 shows the structure of the new adsorbent formed by cross-linking CTS with citrate (ionic cross-linking) and with ECH (covalent cross-linking).

2.4. Adsorption experiment

2.4.1. Effect of pH on the adsorption of metal ions

The effect of the solution pH on the adsorption of Pb (II) and Cu (II) ions onto CTS–CA–ECH beads was studied by shaking 100 mg of dry sample with 50 mL (100 mg L^{-1}) of metal ions solution at predetermined pH and 25 °C for 8 h. The mixed solutions were

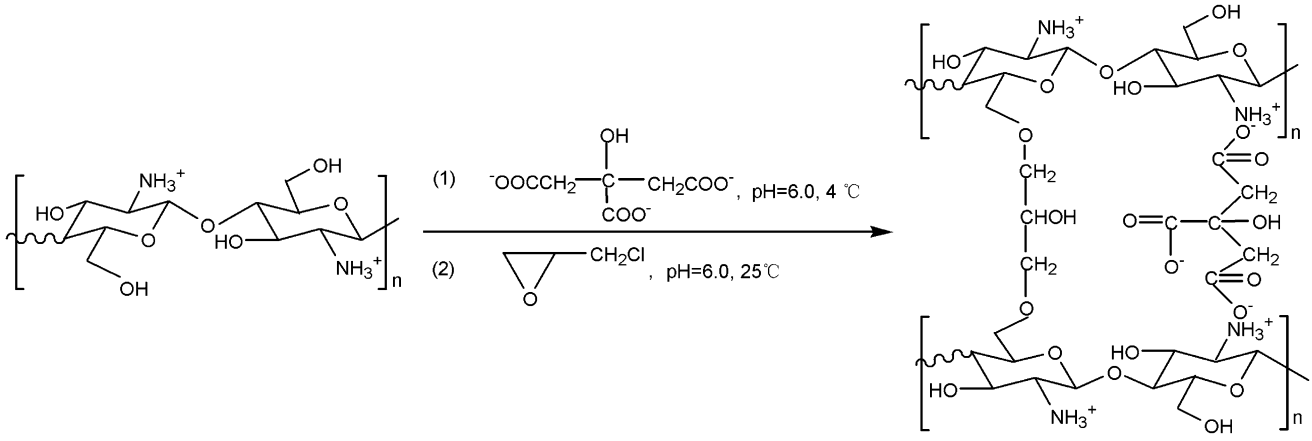

Fig. 1. Scheme for cross-linking CTS with CA and ECH.

buffered within a pH range of 1.0–7.0 to prevent precipitation of Pb (II) and Cu (II) hydroxides occurring at higher pH. After pre-established time periods, the shaking was halted and the beads were filtered. The remaining concentrations of Pb (II) and Cu (II) ions were then determined by FAAS. The adsorption capacity (q_e, mg g^{-1}) was calculated by Eq. (1):

$$q_e = \frac{(C_0 - C_e) \times V}{m} \quad (1)$$

where C_0 is the initial concentration (mg L^{-1}) of metal ions, C_e is the final concentration (mg L^{-1}) of metal ions, V is the volume (mL) of metal ions solution, and m is the mass (mg) of the CTS–CA–ECH beads used.

2.4.2. Effect of temperature on the adsorption of metal ions

The effect of temperature on the adsorption of Pb (II) and Cu (II) ions onto CTS–CA–ECH beads was examined by adding 100 mg of dry sample in a series of flasks containing 50 mL (100 mg L^{-1}) of the metal ions solution at fixed pH. The flasks were shaken on an oscillator at 150 rpm for 8 h under temperatures 25, 30, 35, and 40℃, respectively. After adsorption, each solution was filtered and the remaining concentrations of the metal ions were determined by FAAS.

2.4.3. Effect of contact time on the adsorption of metal ions

The effect of contact time on the adsorption of Pb (II) and Cu (II) ions onto CTS–CA–ECH beads was investigated by adding 100 mg of dry sample in a series of flasks containing 50 mL (100 mg L^{-1}) of metal ion solution at set pH. The flasks were shaken on an oscillator at 150 rpm and 25℃ for a predetermined time period ranging from 20 to 900 min. The remaining metal concentrations of Pb (II) and Cu (II) ions were analyzed as mentioned previously.

2.4.4. Effect of the initial concentration of the metal ions

The effect of initial concentration of Pb (II) and Cu (II) ions on the adsorption onto CTS–CA–ECH beads was carried out by placing 100 mg of dry sample in a series of flasks containing 50 mL of metal ions solution (whose concentrations ranged from 10 to 800 mg L^{-1}) at 25℃ for 8 h under shaking at 150 rpm and at established pH. After adsorption, the solution was filtered and the remaining concentration of the metal ions was determined by FAAS.

2.4.5. Regeneration of adsorbent

Regeneration test was conducted as follows: 100 mg of CTS–CA–ECH beads was loaded with Pb (II) and Cu (II) ions solution (50 mL, 100 mg L^{-1}) at 25℃ for 8 h at set pH, respectively. Afterwards, the metal ions-loaded CTS–CA–ECH beads were collected and washed with distilled water to remove any unadsorbed metal ions. The beads were then shaken with 100 mL of 0.1 mol L^{-1} ethylenediamine tetra-acetic acid (EDTA) solution for 3 h [1,7]. The concentrations of metal ions desorbed into the solution were determined by FAAS. To examine the reusability of the beads, this adsorption–desorption cycle was repeated three times using the same adsorbent.

The desorption percentage (DP) was calculated from the following expression:

$$\mathrm{DP} = \frac{m_d}{m_a} \times 100 \quad (2)$$

where m_a is the amount ($mg\,g^{-1}$) of metal ions adsorbed and m_d is the amount ($mg\,g^{-1}$) of metal ions desorbed.

3. Results and discussion

3.1. Characterization of samples

3.1.1. Thermogravimetric analysis

The TGA thermograms for CTS, CA, and CTS–CA–ECH samples are shown in Fig. 2. For CTS, two degradation stages were included, the first degradation stage was at 42–105°C with a mass loss of about 8%, which can be considered to be the loss of water physically adsorbed on the surface of the materials; the second stage showed that the degradation temperature was 299.1°C with a mass loss of 37.62%. While CA revealed three stages with a total mass loss of about 39.69%. However, in addition to the mass loss of physically adsorbed water, CTS–CA–ECH beads began to sharply degrade at about 209.2°C with a mass loss of about 33.36%, the lower degradation temperature than that of CTS suggested that the new adsorbent was less thermally stable than CTS. The decrease in CTS–CA–ECH stability can be attributed to two reasons. On the one hand, the ionic bonds between the groups $-NH_3^+$ and $-COO^-$ could be dehydrated forming amide bonds –CONH– on heating; on the other hand, the intermolecular and intramolecular hydrogen bonds in original CTS could be reduced due to the formation of covalent bonds and ionic bonds between polymer chains [17].

3.1.2. FTIR analysis

The FTIR spectra for CTS, CTS–CA–ECH, CTS–CA–ECH–Pb(II) and CTS–CA–ECH–Cu (II) are shown in Fig. 3. The peak around 3,400 cm^{-1} for CTS may be attributed to the stretching vibration of –OH and $-NH_2$ groups; the peaks at 1,654 and 1,589 cm^{-1} were due to the N–H stretching and bending vibration in $-NH_2$, respectively; and the peak at 1,421 cm^{-1} represented N–H deformation vibrations. In addition, the peak at 1,376 cm^{-1} was assigned to C–H symmetric bending vibration in $-CH_2OH$; the peaks at 1,323 and 1,155 cm^{-1} were attributed to the C–N stretching vibration; while the peaks at 1,080 and 1,025 cm^{-1} represented the C–O stretching vibrations in –COH [18].

After cross-linking, a shoulder peak at 1,552 cm^{-1} was observed for CTS–CA–ECH with the reduction of the two peaks at 1,654 and 1,589 cm^{-1} due to the existence of NH_3^+; and a new peak at 1,368 cm^{-1} was also found with the disappearance of peaks at 1,421, 1,376, and 1,323 cm^{-1}, which was assigned to $-COO^-$. These peaks suggested the ionic bonds between the protonated amino groups $-NH_3^+$ of CTS and the carboxylic groups $-COO^-$ of CA [7]. Furthermore, it was observed that the peak at 1,025 cm^{-1} disappeared and the intensities at peaks 3,400 and 1,080 cm^{-1} were significantly reduced, indicating that the hydroxyl groups –OH in CTS were involved in the cross-linking process.

After the adsorption of Pb (II) and Cu (II) ions, the major changes in the FTIR spectrum were very similar. This demonstrated that the mechanism for the

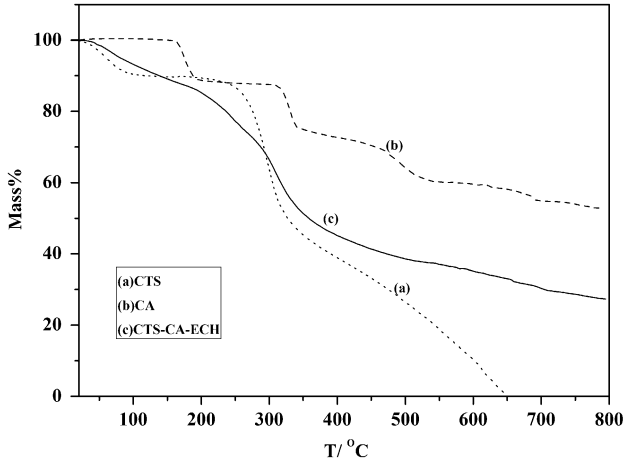

Fig. 2. TGA thermograms of CTS, CA, and CTS–CA–ECH.

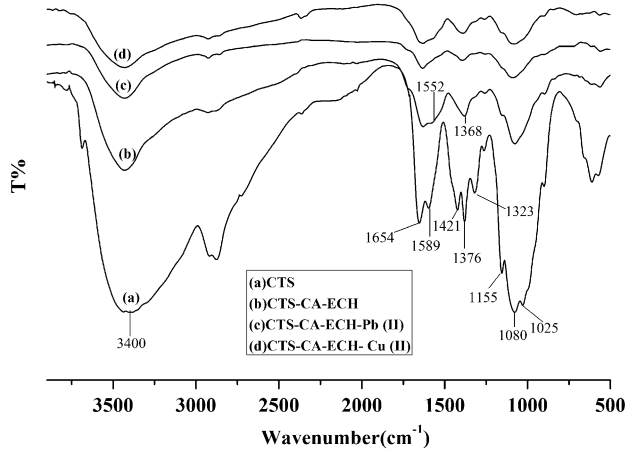

Fig. 3. FTIR of CTS, CTS–CA–ECH, CTS–CA–ECH–Cu (II), and CTS–CA–ECH–Pb (II).

adsorption of the two metal ions were the same. It was observed that the peaks at 3,400 and 1,080 cm^{-1} were further reduced, indicating that the oxygen of hydroxyl groups –OH in cross-linked CTS were involved in the adsorption of metal ions. Meanwhile, there was an obvious reduction at the peak 1,368 cm^{-1}, which indicated that the carboxylic group $–COO^-$ also participated in the adsorption of metal ions.

From the FTIR spectroscopy results, it can be drawn that the cross-linking treatment of CTS with citrate and ECH is successful, and the possible adsorption sites involved in metal ions adsorption could be –OH and $–COO^-$. Fig. 4 is the proposed mechanism for the adsorption of Pb (II) and Cu (II) ions onto CTS–CA–ECH beads.

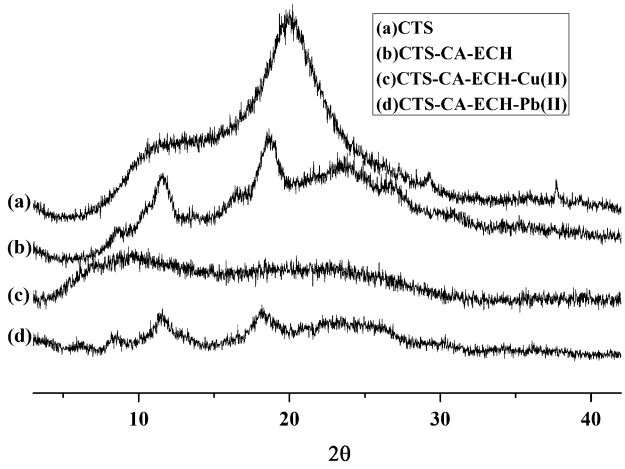

Fig. 5. XRD patterns of CTS, CTS–CA–ECH, CTS–CA–ECH–Cu (II), and CTS–CA–ECH–Pb (II).

3.1.3. XRD analysis

Fig. 5 shows the XRD patterns of CTS, CTS–CA–ECH, and metal ions-loaded CTS–CA–ECH. A typical peak at 19.9° was seen for CTS, which was caused by the hydrogen bonding between hydroxyl groups and amino groups. After cross-linking, the peak at 19.9° became less intense and shifted slightly to a lower angle (about 18.6°) due to the covalent bonds between CTS and ECH and the breaking of hydrogen bonding in CTS, suggesting a decrease in the crystallinity; meanwhile, a new major peak at about 11.5° was clearly observed, which was attributed to the existence of ionic bonds between $–COO^{-1}$ and NH_3^+ as well as the hydrogen bonding between the groups –OH and $–COO^{-1}$, indicating a new crystalline region. However, Cu (II)-loaded CTS–CA–ECH showed significant changes in the main peak characteristics of CTS–CA–ECH, the peak at 11.5° shifted to a lower angle and became broader, and the peak at 18.6° disappeared almost completely owing to the strong coordination of Cu (II) with CTS–CA–ECH and the disruption of hydrogen bonding, illustrating an amorphous structure; while Pb(II)-loaded CTS–CA–ECH obviously reduced the intensity of the peaks at 11.5° and 18.6° to a certain extent, exhibiting weak coordination of Pb (II) with CTS–CA–ECH.

3.2. Effect of pH

Fig. 6 is the effect of pH on the adsorption of Pb (II) and Cu (II) ions by CTS–CA–ECH. It was found that no

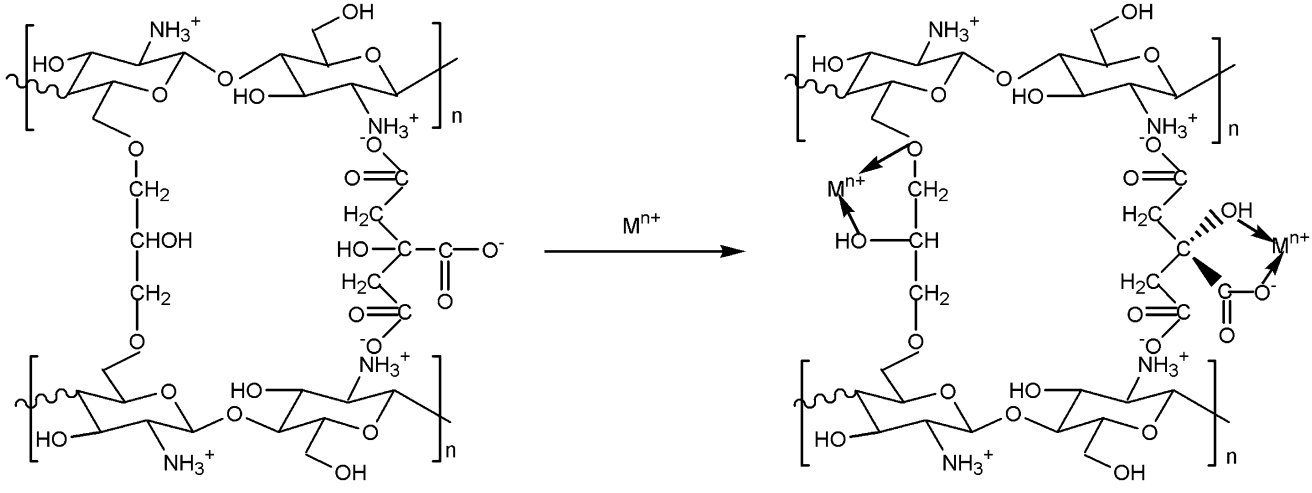

Fig. 4. Proposed mechanism for the adsorption of metal ions by CTS–CA–ECH beads, Mn+ represents Pb (II) or Cu (II) ion.

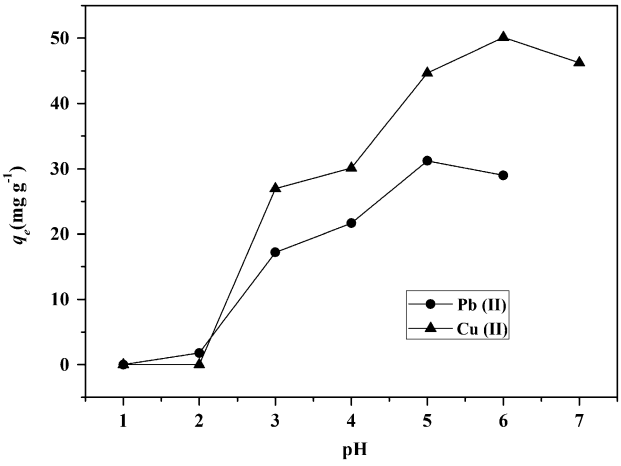

Fig. 6. Effect of pH on the adsorption of Cu (II) and Pb (II) by CTS–CA–ECH (volume = 50 mL; C_0 = 100 mg L^{-1}; adsorbent mass = 100.0 mg; temperature = 25°C; contact time = 8 h).

appreciable uptake was detected for both ions in the pH range of 1.0–2.0. One reason for this was that at such a low pH, the adsorption sites –OH and $–COO^-$ may be completely covered by hydronium ions, which can compete strongly with metal ions for adsorption sites [7,19]; another reason was that the remaining groups $-NH_3^+$ on the surface of the adsorbent (those not formed ionic bonds with $–COO^-$) could generate repulsion to metal ions [20]. However, in the pH range of 2.0–5.0, the adsorption capacity for Pb (II) ions increased with pH; and the same case for Cu (II) ions occurred in the pH range of 2.0–6.0. This was because at higher pH, more adsorption sites were exposed to metal ions and the electrostatic repulsion between adsorbent and metal ions was lowered as some of the groups $-NH_3^+$ were transformed to $-NH_2$ [6,20].

As the pH of Pb (II) ions solution increased from 5.0 to 6.0 and that of Cu (II) ions solution increased from 6.0 to 7.0, the metal ions could be attracted by the increasing hydroxide ions OH^- in solution and had a tendency to form their hydroxide (but the amount of the hydroxide was not enough to produce precipitation yet), thus leading to the decreased adsorption capacity. At higher pH over 7.0, the ionic bonds in CTS–CA–ECH beads could be partially disrupted and precipitation of Pb (II) and Cu (II) hydroxide could appear (for Pb(II) ions solution, at pH over 6.0, a white precipitation can be obviously observed), that may severely affect the adsorption experiments and give inaccurate experimental results. For these reasons, the adsorption experiments at pH over 6.0 for Pb (II) ions and 7.0 for Cu (II) ions were not conducted here.

At pH 5.0 and 6.0, the absorbent showed the maximum adsorption capacity for Pb (II) and Cu (II) ions, respectively. Therefore, the optimum pH for Pb (II) ions adsorption experiment was controlled at pH 5.0 and that for Cu (II) ions was at 6.0 in the present study.

In addition, it was observed that in the studied pH range, the adsorption capacity for Cu (II) ions was higher than that for Pb (II) ions, suggesting possible selectivity for this metal, probably because of its strong coordination with adsorption sites.

3.3. Effect of adsorption temperature

Fig. 7(a) shows the effect of temperature on the adsorption of Cu (II) and Pb (II) ions by CTS–CA–ECH.

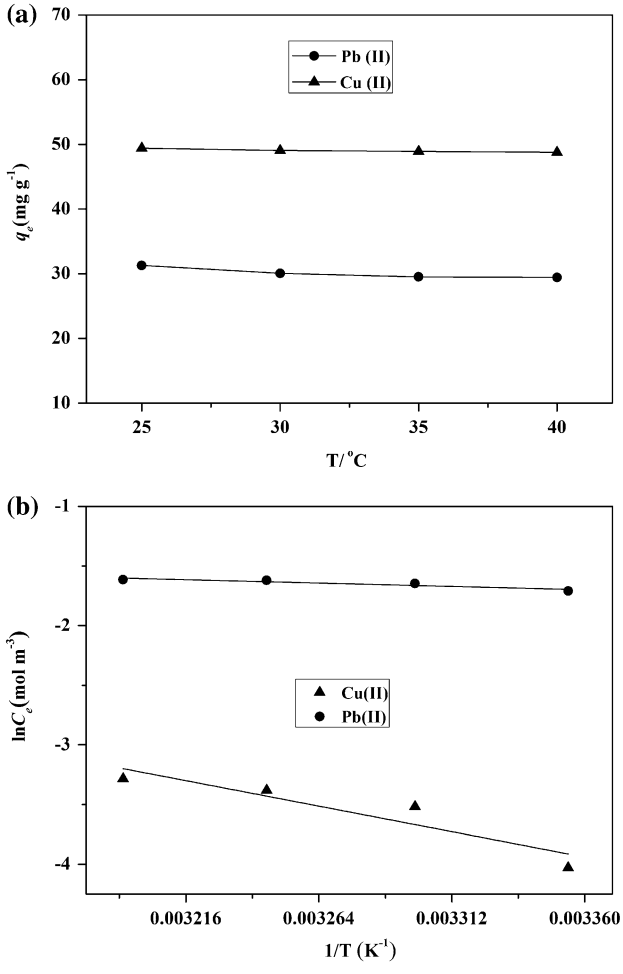

Fig. 7. (a) Effect of temperature on the adsorption of Cu (II) and Pb (II) by CTS–CA–ECH (volume = 50 mL; C_0 = 100 mg L^{-1}; pH = 5.0 for Pb (II) and 6.0 for Cu (II); adsorbent mass = 100.0 mg; contact time = 8 h) and (b) the plot of ln C_e against $1/T$.

It was observed that there was an insignificant decrease in adsorption capacity for both ions with increasing temperature. This can be explained using Clausius–Clapeyron equation [1] as expressed by Eq. (3):

$$\Delta H_x = R\left[\frac{d(\ln C_e)}{d(1/T)}\right] \tag{3}$$

where ΔH_x is the heat of adsorption determined at constant amount of sorbate adsorbed (isosteric heat of adsorption), R is molar gas constant (8.314 J mol^{-1} K^{-1}), and C_e is the equilibrium concentration of the metal ions. ΔH_x is calculated from the slope of the ln C_e vs. $1/T$, as shown in Fig. 7(b). The calculated enthalpy changes were −4.89 and −37.01 kJ mol^{-1} for Pb (II) and Cu (II) ions, respectively. The negative values indicated that the adsorption process was exothermic in nature [1]. This was because two kinds of predominant energy were probably involved in the heat of adsorption. One was consumed to break the hydrogen bonding between adsorption sites for metal ions binding; the other was released during the formation of coordination bonds between metal ions and adsorption sites. Hence, the exothermic adsorption process may be caused by the result that the released energy was more than the consumed. Additionally, the smaller negative value for Pb (II) adsorption may be attributed to its weak coordination with adsorption sites and therefore a lower released energy. Due to the slight effect of temperature on adsorption capacity, for the sake of practicality, all the other adsorption experiments were conducted at room temperature.

3.4. Adsorption kinetics study

To investigate the kinetic mechanism for the adsorption of metal ions by CTS–CA–ECH, the pseudo-first-order (PFO) and pseudo-second-order (PSO) models were applied [21].

The PFO equation is expressed as Eq. (4):

$$\log(q_e - q_t) = \log q_e - \frac{k_1}{2.303}t \tag{4}$$

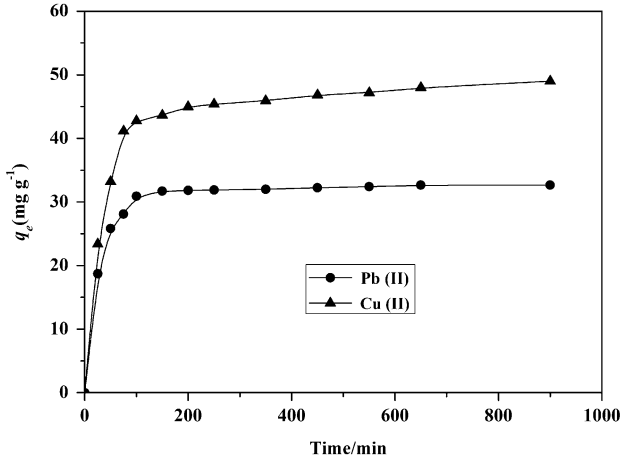

Fig. 8. Effect of contact time on the adsorption of Pb (II) and Cu (II) onto CTS–CA–ECH (volume = 50 mL; C_0 = 100 mg L^{-1}; pH = 5.0 for Pb (II) and 6.0 for Cu (II); adsorbent mass = 100.0 mg; temperature = 25 °C).

where k_1 (min^{-1}) is the rate constant of PFO; q_e (mg g^{-1}) is the equilibrium adsorption capacity; and q_t (mg g^{-1}) is the amount adsorbed at time t (min).

The PSO equation can be expressed as Eq. (5):

$$\frac{t}{q_t} = \frac{1}{k_2 q_e^2} + \frac{t}{q_e} \tag{5}$$

where k_2 (g mg^{-1} min^{-1}) is the rate constant of PSO.

Fig. 8 shows the kinetics of the adsorption for Pb (II) and Cu (II) ions by CTS–CA–ECH. It was observed that the adsorption of Pb (II) and Cu (II) ions were both markedly rapid within the first 75 min, which was resulted from the excessive adsorbing sites available on the surface of the adsorbent. Afterwards, the adsorption increased slowly until the equilibrium for Pb (II) and Cu (II) ions reached in 150 and 200 min, respectively.

The results of the PFO and PSO models for Pb (II) and Cu (II) ions are summarized in Table 1. It could be seen that the PSO model gave higher correlation coefficients (R^2) than the PFO model, and the values of $q_{e,\ cal}$ from the PSO model were very close to the experimental amounts adsorbed ($q_{e,\ exp}$), which were

Table 1
Comparison of kinetic models for the adsorption of Cu (II) and Pb (II) ions by CTS–CA–ECH

Metal ions	$q_{e,exp}$ (mg g^{-1})	PFO			PSO		
		k_1 (min^{-1})	$q_{e,calc}$ (mg g^{-1})	R^2	k_2 (g mg^{-1} min^{-1})	$q_{e,calc}$ (mg g^{-1})	R^2
Cu (II)	49.00	3.22×10^{-3}	11.63	0.8399	8.67×10^{-4}	49.50	0.9995
Pb (II)	32.65	5.76×10^{-3}	4.41	0.8160	6.86×10^{-3}	32.79	0.9999

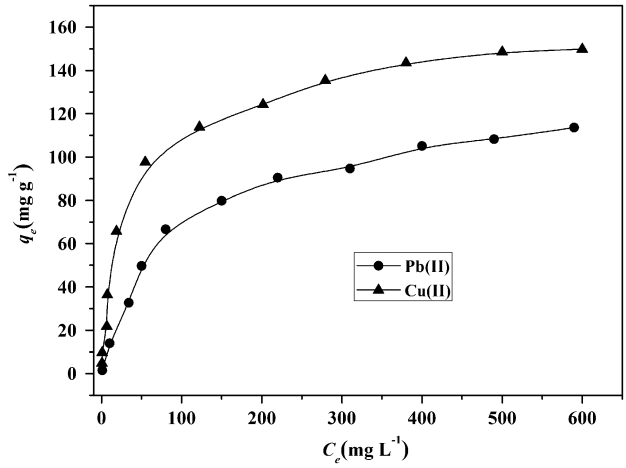

Fig. 9. Adsorption isotherms of Pb (II) and Cu (II) by CTS–CA–ECH (volume = 50 mL; pH = 5.0 for Pb (II) and 6.0 for Cu (II); adsorbent mass = 100.0 mg; temperature = 25 °C; contact time = 8 h).

32.65 and 49.00 mg g^{-1} for Pb (II) and Cu (II) ions, respectively, suggesting that the PSO model was more appropriate to expound the kinetic mechanism than the PFO model. Furthermore, it was found that both the calculated and experimental adsorption amounts for Cu (II) ions were about one and a half times as those for Pb (II) ions, signifying that the modified CTS beads were more preferable to adsorb Cu (II) ions, which could be attributed to the stronger interaction between adsorption sites and Cu (II) ions, as was proved by the results of XRD.

3.5. Equilibrium isotherms study

3.5.1. Langmuir isotherm

The Langmuir model assumes that the adsorbent surface has sites of identical energy and each adsorbate molecule is located at a single site; hence, it predicts the formation of a monolayer of the adsorbate on the adsorbent surface [1,7]. The equation (Eq. (6)) is preferentially used in studies on adsorption in solution.

$$q_e = \frac{K_L C_e q_m}{1 + K_L C_e} \tag{6}$$

And, the linear form of the Langmuir isotherm is expressed as Eq. (7):

$$\frac{C_e}{q_e} = \frac{1}{K_L q_m} + \frac{C_e}{q_m} \tag{7}$$

where q_e (mg g^{-1}) and C_e (mg L^{-1}) are the amount adsorbed and the adsorbate concentration in solution, both at equilibrium, K_L (L g^{-1}) is the Langmuir constant and q_m (mg g^{-1}) is the maximum adsorption capacity for monolayer formation on adsorbent.

3.5.2. Freundlich isotherm

The Freundlich isotherm is an empirical equation and is one of the most widely used isotherms for the description of equilibrium on heterogeneous surfaces [1,7]. Mathematically, it is expressed by Eq. (8):

$$q_e = K_F C_e^{1/n} \tag{8}$$

Eq. (8) can also be expressed as Eq. (9):

$$\ln q_e = \ln K_F + \frac{1}{n} \ln C_e \tag{9}$$

where both K_F and n are Freundlich constants characterizing the adsorption capacity and intensity, respectively.

Fig. 9 shows the experimental equilibrium isotherms for adsorption of Pb (II) and Cu (II) ions on the cross-linked CTS. It was observed that the adsorption capacity increased with the increasing metal ions concentration, progressively saturating the adsorbent. Table 2 lists the isotherm constants of Pb (II) and Cu (II) ions according to the Langmuir and Freundlich isotherm equations. Based on the correlation coefficients (R^2) obtained using the two isotherm models, a conclusion can be drawn that the adsorption of both ions agreed well with the Langmuir isotherm equation

Table 2
Langmuir and Freundlich isotherm parameters for Cu (II) and Pb (II) ions adsorption

Metal ions	Langmuir			Freundlich		
	K_L(L g^{-1})	q_m(mg g^{-1})	R^2	K_F	n	R^2
Cu (II)	3.79×10^{-2}	151.52	0.9947	14.89	2.45	0.8385
Pb (II)	1.26×10^{-2}	121.95	0.9990	2.62	1.55	0.9446

Table 3
Maximum adsorption capacity of various CTS samples modified for adsorption of Cu (II) and Pb (II) ions reported

Adsorbent	q_m(mg g^{-1})		Refs.
	Cu (II)	Pb (II)	
CTS	37.88	13.05	[3]
CTS cross-linked with ECH-TPP	130.72	166.94	[5]
CTS cross-linked with EGDE	45.94	–	[22]
CTS cross-linked with GLA	59.67	–	[22]
CTS cross-linked with ECH	62.47	–	[22]
CTS modified with Reactive Blue 2 dye	57.00	–	[23]
GLA-cross-linked metal-complexed CTS	33.00	105.26	[24]
CTS modified with chloroacetic acid	139.08		[25]
CTS modified with alginate	67.66		[26]
CTS cross-linked with CA–ECH	151.52	121.95	Present study

under the concentration range studied, suggesting a monolayer adsorption.

To evaluate the adsorption ability of the adsorbent toward Pb (II) and Cu (II) ions, it is necessary to compare the data obtained from this study with values from literatures. Table 3 lists the data from various modified CTSs. It can be seen that CTS–CA–ECH showed the highest maximum adsorption capacity for Cu (II) ions and a considerable value for Pb (II) ions. As mentioned before, this unique adsorption behavior of CTS–CA–ECH for Cu (II) ions could be due to the strong coordination between adsorption sites and Cu (II) ions.

3.6. Reuse of adsorbent

For potential practical applications, it is important to examine the possibility of desorbing and regenerating the metal ions-loaded adsorbent. In the present study, EDTA solution (0.1 mol L^{-1}) was chosen to desorb Pb (II) and Cu (II) ions from the adsorbent because of its strong chelating ability toward various metal ions. Table 4 lists the percentages of desorption and the adsorption capacity for Pb (II) and Cu (II) ions in each cycle. It was observed that CTS–CA–ECH beads showed a good desorption performance for Pb (II) and Cu (II) ions and the adsorption capacity for both ions dropped with fewer loss even after three times of recycling use, suggesting that the currently prepared adsorbent possessed an excellent reusability for the adsorption of Pb (II) and Cu (II) ions.

Table 4
Reuse of the new adsorbent CTS–CA–ECH

Cycle number	Pb (II)		Cu (II)	
	q_e (mg g^{-1})	DP	q_e (mg g^{-1})	DP
1	32.65	89.56	49.00	96.32
2	29.89	88.37	48.82	95.52
3	28.38	87.74	47.14	94.36

4. Conclusions

The results of TGA, FTIR, and XRD analysis proved that the novel cross-linked CTS was successfully prepared using CA and ECH as cross-linking agents and the effective adsorption sites of the resulting adsorbent were –OH and –COO^{-1}.

The adsorption of Pb (II) and Cu (II) ions was dependent on the initial solution pH, contact time, and initial concentration of metal ions, while the effect of temperature was slight. The optimum pH values were 5.0 and 6.0 for the adsorption of Pb (II) and Cu (II) ions, respectively, and the equilibrium times for Pb (II) and Cu (II) ions adsorption were 150 and 200 min, respectively.

The kinetics studies indicated that the adsorption of Pb (II) and Cu (II) ions by CTS–CA–ECH followed the PSO model, which gave the best experimental data correlation.

The results of the equilibrium isotherms adsorption for Pb (II) and Cu (II) ions showed that the experimental data fit well with the Langmuir isotherm models, and the maximum adsorption capacities for Pb (II) and Cu (II) ions were 121.95 and 151.52 mg g^{-1}, respectively, suggesting that the obtained adsorbent displayed a good capacity to absorb Pb (II) and Cu (II) ions.

The reuse experiments demonstrated that EDTA could effectively regenerate the Pb (II) and Cu (II)-loaded adsorbent and the currently prepared adsorbent possessed an excellent reusability for the adsorption of Pb (II) and Cu (II) ions.

Acknowledgements

This work was supported by the Fundamental Research Funds (No. 08143079) for the Central University of China.

References

[1] L.M. Zhou, Y.P. Wang, Z.R. Liu, Q.W. Huang, Characteristics of equilibrium, kinetics studies for adsorption of Hg (II), Cu (II), and Ni (II) ions by thiourea-modified magnetic chitosan microspheres, J. Hazard. Mater. 161 (2009) 995–1002.

[2] M.M. Naim, H.E.M. Abdel Razek, Chelation and permeation of heavy metals using affinity membranes from cellulose acetate–chitosan blends, Desalin. Water Treat. 51 (2013) 644–657.
[3] D. Kavak, Removal of lead from aqueous solutions by precipitation: Statistical analysis and modeling, Desalin. Water Treat. 51 (2013) 1720–1726.
[4] A. Shafaei, F.Z. Ashtiani, T. Kaghazchi, Equilibrium studies of the sorption of Hg (II) ions onto chitosan, Chem. Eng. J. 133 (2007) 311–316.
[5] A.H. Chen, S.C. Liu, C.Y. Chen, C.Y. Chen, Comparative adsorption of Cu(II), Zn(II), Pb(II) ions in aqueous solution on the crosslinked chitosan with epichlorohydrin, J. Hazard. Mater. 154 (2008) 184–191.
[6] W.S. Wan Ngah, S. Fatinathan, Pb (II) biosorption using chitosan and chitosan derivatives beads: Equilibrium, ion exchange and mechanism studies, J. Environ. Sci. 22(3) (2010) 338–346.
[7] R. Laus, T.G. Costa, B. Szpoganicz, V.T. Fávere, Adsorption and desorption of Cu(II), Cd(II) and Pb(II) ions using chitosan crosslinked with epichlorohydrin–triphosphate as the adsorbent, J. Hazard. Mater. 183 (2010) 233–241.
[8] M.S. Chiou, H.Y. Li, Adsorption behavior of reactive dye in aqueous solution on chemical cross-linked chitosan beads, Chemosphere 50 (2003) 1095–1105.
[9] H.L. Vasconcelos, T.P. Camargo, N.S. Goncalves, A. Neves, M.C.M. Laranjeira, V.T. Fávere, Chitosan crosslinked with a metal complexing agent: Synthesis, characterization and copper (II) ions adsorption, React. Funct. Polym. 68 (2008) 572–579.
[10] E. Guibal, Interactions of metal ions with chitosan-based sorbents: A review, Sep. Purif. Technol. 38 (2004) 43–74.
[11] V.L. Gon alves, M.C.M. Laranjeira, V.T. Fávere, R.C. Pedrosa, Effect of crosslinking agents on chitosan microspheres in controlled release of diclofenac sodium, Polímeros 15 (2005) 6–12.
[12] W.S. Wan Ngan, M.A.K.M. Hanafiah, S.S. Yong, Adsorption of humic acid from aqueous solution on crosslinked chitosan–epichlorohydrin beads: Kinetics and isotherm studies, Colloids Surf. B. 65 (2008) 18–24.
[13] S.T. Lee, F.L. Mi, Y.J. Shen, S.S. Shyu, Equilibrium and kinetic studies of copper (II) ion uptake by chitosan–tripolyphosphate chelating resin, Polymer 42 (2001) 1879–1892.
[14] J.H. Park, D. Jung, Removal of total phosphorus (TP) from municipal wastewater using loess, Desalination 269 (2011) 104–110.
[15] X.Z. Shu, K.J. Zhu, W.H. Song, Novel pH-sensitive citrate cross-linked chitosan film for drug controlled release, Int. J. Pharm. 212 (2001) 19–28.
[16] M.M. Beppu, R.S. Vieira, C.G. Aimoli, C.C. Santana, Crosslinking of chitosan membranes using glutaraldehyde: Effect on ion permeability and water adsorption, J. Membr. Sci. 301 (2007) 126–130.
[17] R. Laus, V.T. de Fávere, Competitive adsorption of Cu (II) and Cd(II) ions by chitosan crosslinked with epichlorohydrin–triphosphate, Bioresour. Technol. 102 (2011) 8769–8776.
[18] N. Li, R.B. Bai, A novel amine-shielded surface crosslinking of chitosan hydrogel beads for enhanced metal adsorption performance, Ind. Eng. Chem. Res. 44 (2005) 6692–6700.
[19] S.S. Gupta, K.G. Bhattacharyya, Adsorption of Ni (II) on clays, J. Colloid Interface Sci. 295 (2006) 21–32.
[20] W.S. Wan Ngah, S. Fatinathan, Adsorption characterization of Pb (II) and Cu (II) ions onto chitosan–tripolyphosphate beads: Kinetic, equilibrium and thermodynamic studies, J. Environ. Manage. 91 (2010) 958–969.
[21] F.C. Wu, R.L. Tseng, R.S. Juang, Kinetic modeling of liquid-phase adsorption of reactive dyes and metal ions on chitosan, Water Res. 35 (2001) 613–618.
[22] W.S. Wan Ngah, C.S. Endun, R. Mayanar, Removal of copper (II) ions from aqueous solution onto chitosan and cross-linked chitosan beads, React. Funct. Polym. 50 (2002) 181–190.
[23] H.L. Vasconcelos, V.T. Fávere, N.S. Gon alves, M.C.M. Laranjieira, Chitosan modified with Reactive Blue 2 dye on adsorption equilibrium of Cu (II) and Ni (II) ions, React. Funct. Polym. 67 (2007) 1052–1060.
[24] A.H. Chen, C.Y. Yang, C.Y. Chen, C.W. Chen, The chemically crosslinked metal-complexed chitosan for comparative adsorption of Cu (II), Zn(II), Ni (II) and Pb(II) ions in aqueous medium, J. Hazard. Mater. 163 (2009) 1068–1075.
[25] H. Yan, J. Dai, Z. Yang, H. Yang, R.S. Cheng, Enhanced and selective adsorption of copper (II) ions on surface carboxymethylated chitosan hydrogel beads, Chem. Eng. J. 174 (2011) 586–594.
[26] W.S. Wan Ngah, S. Fatinathan, Adsorption of Cu (II) ions in aqueous solution using chitosan beads, chitosan–GLA beads and chitosan–alginate beads, Chem. Eng. J. 143 (2008) 62–72.